HAL
archives-ouvertes.fr

Euclidean Structure from N>=2 Parallel Circles: Theory and Algorithms

Pierre Gurdjos, Peter Sturm, Yihong Wu

▶ To cite this version:

Pierre Gurdjos, Peter Sturm, Yihong Wu. Euclidean Structure from N>=2 Parallel Circles: Theory and Algorithms. European Conference on Computer Vision, May 2006, Graz, Austria. pp.238-252, 2006. <inria-00387126>

HAL Id: inria-00387126
https://hal.inria.fr/inria-00387126

Submitted on 24 May 2009

Euclidean Structure from $N \geq 2$ Parallel Circles: Theory and Algorithms

Pierre Gurdjos[1], Peter Sturm[2], and Yihong Wu[3]

[1] IRIT-TCI, UPS, 118 route de Narbonne,
31062 Toulouse, cedex 9, France
Pierre.Gurdjos@irit.fr
[2] PERCEPTION, INRIA Rhône-Alpes,
655, avenue de l'Europe, 38330 Montbonnot, France
Peter.Sturm@inrialpes.fr
[3] NLPR-IA, Chinese Academy of Sciences, P.O. Box 2728,
No. 95 East Road of Zhong Guan Cun, Beijing 100080, China
yhwu@nlpr.ia.ac.cn

Abstract. Our problem is that of recovering, in one view, the 2D Euclidean structure, induced by the projections of N parallel circles. This structure is a prerequisite for camera calibration and pose computation. Until now, no general method has been described for $N > 2$. The main contribution of this work is to state the problem in terms of a system of linear equations to solve. We give a closed-form solution as well as bundle adjustment-like refinements, increasing the technical applicability and numerical stability. Our theoretical approach generalizes and extends all those described in existing works for $N = 2$ in several respects, as we can treat simultaneously pairs of orthogonal lines and pairs of circles within a unified framework. The proposed algorithm may be easily implemented, using well-known numerical algorithms. Its performance is illustrated by simulations and experiments with real images.

1 Introduction

The roles played by quadrics and conics in recovering the Euclidean structure of a 3D world have been widely investigated in the computer vision literature [1][3][12][15][17][19]. More generally, it is now well-understood that the keys to Euclidean structures [6][11][13][14][17][19][23], in the considered d-dimensional space, are the identifications of *absolute* entities, typically *absolute* quadrics and conics, whose characteristics are to be left invariant under similarities in d-space. As an example, the absolute disk quadric envelope, introduced by Triggs in [22], encodes the complete Euclidean structure of the 3D space.

In the specific case of a 2D scene, located on some 3D supporting plane π, the image plane of a pinhole camera, to which is projected the scene, can be seen as a projective representation of π. Formally speaking, the 2D Euclidean structure of π is given by two (projected) *absolute* conjugate complex points, so-called (projected) circular points [5][18]. The circular points of π are, by definition, common to all of its circles. It is therefore not surprising that the issue of

inferring metric properties about the camera and/or the scene, from projections of circular features has been considered, especially for camera calibration purposes [3][11][13][19][23]. Intrinsically, circular targets offer arguably interesting visual clues: they can be easily detected and fitted [7], even if partially occluded. It is nevertheless worth remembering that the sole knowledge of the 2D Euclidean structure of π w.r.t. one view is insufficient for calibrating the camera and recovering the 3D pose of π i.e., multiple views are required [20][22][24].

In this work, we are aiming at finding a closed-form solution to the problem of recovering such a 2D Euclidean structure, common to a family of parallel planes, from $N \geq 2$ projected unknown parallel circles. Until now, this only has been solved (in these terms) for $N = 2$. We emphasize the fact that circles may correspond to physical entities, like external parallels of a surface of revolution [6], but also to virtual ones e.g., the para-catadioptric projection of a line onto the mirror surface [2], the circular motion of a 3D point [11] or even the absolute conic [10, pp. 81-83], which makes this problem of broader interest.

Our theoretical approach, giving new geometrical insights, unifies and generalizes those described in prior works for $N = 2$ in several respects. We propose:

- a rigorous formalism, based on the projective invariance of absolute signatures of degenerate circles and generalized eigenvalues of circle pencils;
- a linear algorithm for $N \geq 2$ circles, that yields a closed-form solution and optimal (non-linear) refinements; it generalizes [14, p.60], by the ability of treating simultaneously pairs of orthogonal lines and pairs of circles.

2 Problem statement and proposed interpretation

Our problem, so-called P_N, is that of recovering the Euclidean structure, common to a family of parallel planes, from N projected circles in one view, taken by an uncalibrated camera. By *projected circles*, we refer to conics of the image plane $\tilde{\pi}$, which are the projections of 3D *parallel circles* i.e., lying on parallel planes. Let h denote the world-to-image homography, mapping one of these plane, say π, to the image plane $\tilde{\pi}$. Since the pre-image $\mathcal{A} \equiv h^{-1}(\tilde{\mathcal{A}})$ of any projected circle $\tilde{\mathcal{A}}$ is always a circle in π, for the sake of simplicity, we will only consider as world circles, not all 3D parallel circles, but the corresponding coplanar circles of π. Hence, we restrict the terms circles to only refer *coplanar circles*.

To solve P_N, all we have at our disposal are the symmetric image matrices $\tilde{\mathbf{A}}_j \in \mathbb{R}^{3 \times 3}$ of $N \geq 2$ projections $\tilde{\mathcal{A}}_j$ of circles $\mathcal{A}_j$ of π, $j = 2..N$. The problem P_2 i.e., for $N = 2$, can be simply stated e.g., as in [6][11][23]. The Euclidean structure of π is encoded by its projected circular points $\tilde{\mathtt{I}} \equiv h(\mathtt{I})$, $\tilde{\mathtt{J}} \equiv h(\mathtt{J})$, where the circular points $\mathtt{I}$, $\mathtt{J}$ are, by definition [5][18], common to all circles, including the absolute conic. Hence, two projected circles have four points in common, among which is the point-pair $(\tilde{\mathtt{I}}, \tilde{\mathtt{J}})$. The other point-pair, denoted here by $(\tilde{\mathtt{G}}, \tilde{\mathtt{H}})$, consists of either real or conjugate complex points. Both point-pairs span real lines, namely the vanishing line $\tilde{\mathsf{L}}_\infty \equiv h(\mathsf{L}_\infty)$ and some "other" line $\tilde{\Delta} \equiv h(\Delta)$. The existing algorithms solving P_2 basically work as follows: (i) they compute the four common points of $\tilde{\mathcal{A}}_1$, $\tilde{\mathcal{A}}_2$; (ii) they pick up the projected

circular point-pair $(\check{\mathtt{I}}, \check{\mathtt{J}})$. Regarding (ii), when the two obtained point-pairs are conjugate complex, it can be required to first determine which line is $\check{\mathsf{L}}_\infty$ i.e., is the line spanned by $(\tilde{\mathtt{I}}, \tilde{\mathtt{J}})$. These algorithms were designed to only deal with two circles and their extensions to multiple circles is clearly troublesome. Indeed, for $N > 2$, it is about estimating the common root of multiple degree-4 polynomials. Thus, the issue of finding a numerically stable closed-form solution is far from straightforward.

Consider a set of $N \geq 2$ projected circles. An elegant means of solving the problem P_N is to interpret all or some pairs of the set of projected circles as "generators" of pencils of conics [5][17][18]. This is the basic idea of the proposed work. Let us say that $(\tilde{\mathcal{A}}_1, \tilde{\mathcal{A}}_2)$ is one of these pairs, spanning the conic pencil $\{\tilde{\mathcal{A}}_1, \tilde{\mathcal{A}}_2\}$. This latter is the linear family of projected circles, with image matrices $\tilde{\mathbf{A}}(\tilde{\lambda}) \equiv \tilde{\mathbf{A}}_1 - \tilde{\lambda}\tilde{\mathbf{A}}_2$, where $\tilde{\mathbf{A}}$ is the image matrix of $\tilde{\mathcal{A}}$ and $\tilde{\lambda} \in \mathbb{C}$ is a parameter. It includes three *degenerate conics consisting of line-pairs*, whose parameters $\tilde{\lambda}_k$, $k = 1..3$, are the generalized eigenvalues of $(\tilde{\mathbf{A}}_1, \tilde{\mathbf{A}}_2)$. If $\tilde{\mathbf{p}} \in \mathbb{C}^3$ represents any of the four common points of $\tilde{\mathcal{A}}_1$ and $\tilde{\mathcal{A}}_2$, then the equation $\tilde{\mathbf{p}}^\top \tilde{\mathbf{A}}_1 \tilde{\mathbf{p}} = 0$ holds as well as $\tilde{\mathbf{p}}^\top \tilde{\mathbf{A}}_2 \tilde{\mathbf{p}} = 0$. Thus, taking any linear combination for one of the generalized eigenvalues $\tilde{\lambda}_k$, the equation $\tilde{\mathbf{p}}^\top (\tilde{\mathbf{A}}_1 - \tilde{\lambda}_k \tilde{\mathbf{A}}_2)\tilde{\mathbf{p}} = 0$ also holds. This means that the projected circular points $\tilde{\mathtt{I}}, \tilde{\mathtt{J}}$ lie on *all* the projected degenerate conics of the pencil, which so are projected *degenerate circles*. Therefore, by considering multiple projected circle-pairs, this reduces the problem of recovering $\tilde{\mathtt{I}}, \tilde{\mathtt{J}}$ to basically that of finding the (complex) intersection of a set of lines (cf. Fig. 1). A closed-form solution can then be obtained using a *linear algorithm* i.e., by solving an overdetermined system of linear equations.

This proposed interpretation will also allow us to exhibit interesting results. It can be shown that one of the degenerate members of the pencil $\{\tilde{\mathcal{A}}_1, \tilde{\mathcal{A}}_2\}$ is the projected degenerate circle $\widetilde{\Delta \mathsf{L}_\infty}$ i.e., consisting of the two lines $\tilde{\Delta}$ and $\tilde{\mathsf{L}}_\infty$, where $\tilde{\mathsf{L}}_\infty$ is the vanishing line of π. An important fact is that $\widetilde{\Delta \mathsf{L}_\infty}$ can always be distinguished from the other degenerate members, thanks to a discriminant invariant *absolute signature* (cf. §3.1). Because our algorithm requires to distinguish $\tilde{\mathsf{L}}_\infty$ from $\tilde{\Delta}$, in §4.3, we will put the emphasis on the roles played by the projections $\check{\mathsf{Z}}_1 = h(\mathsf{Z}_1)$ and $\check{\mathsf{Z}}_2 = h(\mathsf{Z}_2)$ of the so-called *limiting points* of the pencil $\{\tilde{\mathcal{A}}_1, \tilde{\mathcal{A}}_2\}$, whose image vectors correspond to two (identifiable) generalized eigenvectors of $(\tilde{\mathbf{A}}_1, \tilde{\mathbf{A}}_2)$. Specifically, we will be able to establish a general necessary and sufficient condition, cf. Propr. 1, depending on the relative positions of $\check{\mathsf{Z}}_1, \check{\mathsf{Z}}_2$ w.r.t. $\check{\Delta}$, for problem P_2 to be well-posed i.e., for the Euclidean structure to be recovered. In particular, we will show there exist enclosing but not concentric circle-pairs (as shown in Fig. 2) for which the condition holds, contrary to what was previously claimed in [11][23].

3 Some projective and Euclidean properties of conics

Before going more into detail about our problem P_N, we state some properties of conics relevant to our work. General projective properties of conics and their

envelopes can be found in standard textbooks, such as [18]. In this section, we restrict the term conics to only refer *coplanar conics*.

Throughout §3-§4, for the sake of simplicity, we will deal with two different 2D representations of a supporting plane, namely Euclidean and projective. The former can be seen as the world representation and the latter as the image representation. When referring to the vectors/matrices of entities w.r.t. the projective representation, we will systematically add the symbol ˜, like in (1). We ask the reader to keep in mind that $\mathbf{Q}$ and $\tilde{\mathbf{Q}}$ will represent the same entity $\mathcal{Q}$ until §5.

The dual notion of a (point) conic $\mathcal{Q}$, represented by the symmetric matrix $\mathbf{Q} \in \mathbb{R}^{3\times3}$, is the (line) conic envelope $\mathcal{Q}^*$, whose matrix is the adjugate matrix[4] $\mathbf{Q}^*$. The *projective matrix* $\tilde{\mathbf{Q}}$ of a conic $\mathcal{Q}$ is related to the *Euclidean matrix* $\mathbf{Q}$ of $\mathcal{Q}$ by the congruence:

$$\tilde{\mathbf{Q}} = s\mathbf{H}^{-\top}\mathbf{Q}\mathbf{H}^{-1}, \ s \neq 0, \tag{1}$$

where $\mathbf{H} \in \mathbb{R}^{3\times3}$ is the matrix of the Euclidean-to-projective homography.

3.1 Projectively invariant classification of degenerate conics

We let the reader dually restate the following results, by substituting point for line as well as envelope for locus, whenever the sans serif font is used.

A degenerate conic locus consists of either two lines M and N, with vectors $\tilde{\mathbf{m}}$ and $\tilde{\mathbf{n}}$, such that its matrix satisfies $\tilde{\mathbf{D}} \sim \tilde{\mathbf{m}}\tilde{\mathbf{n}}^\top + \tilde{\mathbf{n}}\tilde{\mathbf{m}}^\top$, or a repeated line M = N such that $\tilde{\mathbf{D}} \sim \tilde{\mathbf{m}}\tilde{\mathbf{m}}^\top$. If M ≠ N i.e., rank($\tilde{\mathbf{D}}$) = 2, then $\tilde{\mathbf{m}} \times \tilde{\mathbf{n}} \in \text{null}\,\tilde{\mathbf{D}}$.

We will now focus on degenerate conics $\mathcal{D}$, whose matrices $\tilde{\mathbf{D}}$ are real. They obey to a projectively invariant classification, thanks to the following properties.

For any singular $\tilde{\mathbf{D}} \in \mathbb{R}^{3\times3}$, define the **absolute signature** $\Sigma(\tilde{\mathbf{D}}) \equiv |\eta - \nu|$, where η and ν count the positive and negative eigenvalues of $\tilde{\mathbf{D}}$. As a corollary of Sylvester's inertia theorem [9, p. 403], it can be established that $\Sigma(\tilde{\mathbf{D}}) \equiv |\eta - \nu|$ is invariant under congruence transformations of $\tilde{\mathbf{D}}$, as is rank $\tilde{\mathbf{D}} \equiv \eta + \nu$, which entails that both the absolute signature and the rank of $\mathcal{D}$ are projectively invariant. It is then easy to show that:

$$\Sigma(\tilde{\mathbf{D}}) = \begin{cases} 0 \Leftrightarrow \{\tilde{\mathbf{m}}, \tilde{\mathbf{n}}\} = \{\tilde{\mathbf{x}}_1 + \tilde{\mathbf{x}}_2, \tilde{\mathbf{x}}_1 - \tilde{\mathbf{x}}_2\} & \text{iff M, N are } \textit{real} \text{ and } \textit{distinct} \\ 1 \Leftrightarrow \tilde{\mathbf{m}} = \tilde{\mathbf{n}} = \tilde{\mathbf{x}}_1 & \text{iff M = N is } \textit{real} \\ 2 \Leftrightarrow \{\tilde{\mathbf{m}}, \tilde{\mathbf{n}}\} = \{\tilde{\mathbf{x}}_1 + i\tilde{\mathbf{x}}_2, \tilde{\mathbf{x}}_1 - i\tilde{\mathbf{x}}_2\} & \text{iff M, N are } \textit{conjugate complex} \end{cases}$$

$$\text{where } \begin{bmatrix} \tilde{\mathbf{x}}_1 & \tilde{\mathbf{x}}_2 \end{bmatrix} \equiv \mathbf{U}\mathbf{S}^{1/2} \begin{bmatrix} \mathbf{e}_1 & \mathbf{e}_2 \end{bmatrix} \in \mathbb{R}^{3\times2} \tag{2}$$

involves the SVD [9, p. 70] $\mathbf{U}^\top\tilde{\mathbf{D}}\mathbf{V} = \text{diag}(s_1, s_2, 0) \equiv \mathbf{S}$, for orthogonal $\mathbf{U}$, $\mathbf{V} \in \mathbb{R}^{3\times3}$, with singular values $s_1 > s_2 \geq 0$, and $\mathbf{e}_1 \equiv (1,0,0)^\top$, $\mathbf{e}_2 \equiv (0,1,0)^\top$.

3.2 Euclidean structure and circular-point envelope

In the light of §3.1, the "absolute" degenerate conic that will be central regarding our problem is the **circular-point envelope** IJ, consisting of the circular point-pair. It encodes the Euclidean structure in 2D space, in much the same way as

---

[4] If $\mathbf{Q}$ is not degenerate, then then $\mathbf{Q}^* \equiv \det(\mathbf{Q})\mathbf{Q}^{-1}$

the degenerate absolute quadric envelope [21], encodes the Euclidean structure in 3D space. Thus, IJ is left invariant under 2D similarities.

The only "tangent" that touches IJ at both circular points is L_∞, such that (3a) holds. The other "tangents" touch IJ at one circular point and are isotropic lines. An **isotropic line** is the complex line, denoted by C^I (resp. C^J), through a real finite point C and I (resp. J), with conjugate complex vectors $\tilde{\mathbf{x}}_1 + i\tilde{\mathbf{x}}_2$ (resp. $\tilde{\mathbf{x}}_1 - i\tilde{\mathbf{x}}_2$). They are *self-perpendicular lines*, satisfying (3b). *Perpendicular lines* M and N, with vectors $\tilde{\mathbf{m}}$ and $\tilde{\mathbf{n}}$, are conjugate w.r.t. IJ, satisfying (3c).

$$\tilde{\mathbf{C}}_\infty^* \tilde{\mathbf{l}}_\infty = \mathbf{0}_3, \tag{3a}$$

$$\tilde{\mathbf{x}}_1^\top \tilde{\mathbf{C}}_\infty^* \tilde{\mathbf{x}}_2 = 0 \quad \text{and} \quad \tilde{\mathbf{x}}_1^\top \tilde{\mathbf{C}}_\infty^* \tilde{\mathbf{x}}_1 - \tilde{\mathbf{x}}_1^\top \tilde{\mathbf{C}}_\infty^* \tilde{\mathbf{x}}_2 = 0, \tag{3b}$$

$$\tilde{\mathbf{m}}^\top \tilde{\mathbf{C}}_\infty^* \tilde{\mathbf{n}} = 0. \tag{3c}$$

Equations (3a), resp. (3b)-(3c), describe affine, resp. Euclidean, constraints on IJ, with rank-2 matrix $\tilde{\mathbf{C}}_\infty^*$.

4 Linear Euclidean constraints from $N \geq 2$ circles

### 4.1 Treating two circles as generators of a pencil of circles

As said before, interpreting all or some circle-pairs as generators of pencils of circles [5][18] offers an elegant means of extending the algorithm from $N = 2$ to $N > 2$ circles. The conic pencil $\{\mathcal{A}_1, \mathcal{A}_2\}$, with circle-pair $(\mathcal{A}_1, \mathcal{A}_2)$ as generators, is the linear family of circles, with matrices of the form $\tilde{\mathbf{A}}(\tilde{\lambda}) \equiv \tilde{\mathbf{A}}_1 - \tilde{\lambda}\tilde{\mathbf{A}}_2$. There are three degenerate circles in $\{\mathcal{A}_1, \mathcal{A}_2\}$, whose parameters $\tilde{\lambda}$ are the generalized eigenvalues of $(\tilde{\mathbf{A}}_1, \tilde{\mathbf{A}}_2)$.

In this work, we *only* consider non-intersecting generators[5]. As a consequence, any degenerate circles of $\{\mathcal{A}_1, \mathcal{A}_2\}$ have a real rank-2 matrix so can be classified and decomposed into lines, according to (2). Remind that the Euclidean structure of π is encoded by the circular-point envelope IJ, as explained in §3.2. The important fact is that a degenerate circle of $\{\mathcal{A}_1, \mathcal{A}_2\}$ is either an isotropic line-pair, through I and J, or a real line-pair, including L_∞. In the former case, we call it **point-circle**, yielding Euclidean constraints (3b) on the plane's structure IJ. In the latter, we call it **line-circle**, yielding, providing L_∞ is identified, affine constraints (3a). Identifying L_∞ is about distinguishing its vector in decomposition (2). As explained in [23], solving this ambiguity requires to study the relative position of $\mathcal{A}_1$ and $\mathcal{A}_2$.

4.2 Relative positions of two circles and generalized eigenvalues

The issue of studying the different relative positions of $\mathcal{A}_1$ and $\mathcal{A}_2$ is now tackled by analysing the generalized eigenvalues [9, p. 375] of $(\tilde{\mathbf{A}}_1, \tilde{\mathbf{A}}_2)$, which are the three real solutions for $\tilde{\lambda}$ of the cubic equation $\det(\tilde{\mathbf{A}}_1 - \tilde{\lambda}\tilde{\mathbf{A}}_2) = 0$.

---

[5] Actually, the case of intersecting circles does not introduce major difficulties to be treated in the proposed framework, besides dealing with complex generalized eigenvalues. However, owing to lack of space, this could hardly be included here.
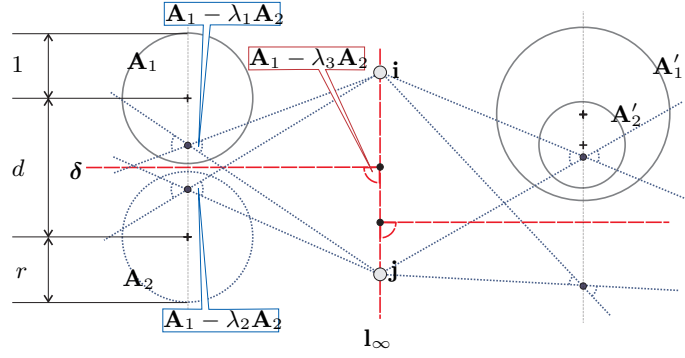
Fig. 1. The problem of finding the circular points may reduce to that of intersecting degenerate circles, consisting of line-pairs, with rank-2 matrices of the form $\mathbf{A}_1 - \lambda \mathbf{A}_2$.

An interesting fact is that the generalized eigenvalues are projectively invariant as a set, up to a scale factor [16]. More precisely, if $\tilde{\mathbf{A}}_j = s_j \mathbf{H}^{-\top} \mathbf{A}_j \mathbf{H}^{-1}$, then $(\tilde{\lambda}, \mathbf{z})$ and $(\frac{s_2}{s_1}\tilde{\lambda}, \mathbf{H}\mathbf{z})$ are generalized eigen-pairs of $(\mathbf{A}_1, \mathbf{A}_2)$ and $(\tilde{\mathbf{A}}_1, \tilde{\mathbf{A}}_2)$, respectively. This allows us to introduce canonical matrices in order to simplify computations.

Let us attach some Euclidean representation to the 3D plane such that $\mathcal{A}_1$ and $\mathcal{A}_2$ have (Euclidean) matrices:

$$\mathbf{A}_1 = \begin{bmatrix} 1 & 0 & 0 \\ 0 & 1 & 0 \\ 0 & 0 & -1 \end{bmatrix}, \ \mathbf{A}_2 = \begin{bmatrix} 1 & 0 & -d \\ 0 & 1 & 0 \\ -d & 0 & d^2 - r^2 \end{bmatrix}. \tag{4}$$

Thus, $\mathcal{A}_1$ is centred at the origin $\mathbf{O}$ and has radius 1; $\mathcal{A}_2$ is centred at point $(0, d)$, with $d \geq 0$, and has radius $r > 0$ (cf. Fig. 1).

We can specify all relative positions of $\mathcal{A}_1$, $\mathcal{A}_2$, using constraints on d and r. Circles **intersect** (i.e., at *two* real points) iff $d > |r - 1|$ *and* $d < r + 1$, or, equivalently, iff $\alpha < 0$, where:

$$\alpha \equiv (d - r + 1)(d - r - 1)(d + r - 1). \tag{5}$$

Regarding other cases, $\mathcal{A}_1$ and $\mathcal{A}_2$ are **tangent** iff $\alpha = 0$ and are **disjoint** i.e., not intersecting, iff $\alpha > 0$. Disjoint circles can be **separate** $(d > r + 1)$, **concentric** $(d = 0)$ or **enclosing but not concentric** $(d < |r - 1|)$.

What the generalized eigenvalues of $(\tilde{\mathbf{A}}_1, \tilde{\mathbf{A}}_2)$ tell us. We now explain how to recover d and r from the generalized eigenvalues of $(\tilde{\mathbf{A}}_1, \tilde{\mathbf{A}}_2)$ and, thus, how to determine the relative position of the generators $\mathcal{A}_1$, $\mathcal{A}_2$.

Let $\tilde{\boldsymbol{\lambda}}$, resp. $\boldsymbol{\lambda}$, denote the vector of generalized eigenvalues of $(\tilde{\mathbf{A}}_1, \tilde{\mathbf{A}}_2)$, resp. $(\mathbf{A}_1, \mathbf{A}_2)$, computed by MAPLE as:

$$\tilde{\boldsymbol{\lambda}} \sim \boldsymbol{\lambda} = \left(\frac{1 + r^2 - d^2 - \sqrt{\beta}}{2r^2}, \ \frac{1 + r^2 - d^2 + \sqrt{\beta}}{2r^2}, \ 1 \right)^\top, \quad \beta \equiv \alpha(d + r + 1). \tag{6}$$

Since we deal with non-intersecting generators, we have $\alpha \geq 0 \Rightarrow \beta \geq 0$. Therefore, all the λ's are real so all the degenerate circles have real matrices.

Now, consider the system of two equations obtained by expanding and simplifying $(\tilde{\lambda}_1 \pm \tilde{\lambda}_2)/\tilde{\lambda}_3$, in order to eliminate the scale factor in $\tilde{\boldsymbol{\lambda}}$. Then, solve it for d and r by only picking the positive values. We get:

$$
\begin{cases} (\tilde{\lambda}_1 + \tilde{\lambda}_2)/\tilde{\lambda}_3 = (r^2 - d^2 + 1)/r^2 \\ (\tilde{\lambda}_1 - \tilde{\lambda}_2)/\tilde{\lambda}_3 = \sqrt{\beta}/r^2 \end{cases} \Leftrightarrow \begin{cases} d = \sqrt{\tilde{\lambda}_1 \tilde{\lambda}_2 (\tilde{\lambda}_1 - \tilde{\lambda}_3)(\tilde{\lambda}_2 - \tilde{\lambda}_3)}/|\tilde{\lambda}_1 \tilde{\lambda}_2| \\ r = |\tilde{\lambda}_3|/\sqrt{\tilde{\lambda}_1 \tilde{\lambda}_2} \end{cases}
$$
(7)

Ordering the generalized eigenvalues. Since $\tilde{\lambda}_1$, $\tilde{\lambda}_2$ play symmetric roles in (7), do not distinguish them by using indifferently the notations $\tilde{\lambda}_+$ or $\tilde{\lambda}_-$. Moreover, denote by $\Sigma(\tilde{\lambda})$ the absolute signature $\Sigma(\tilde{\mathbf{A}}_1 - \tilde{\lambda}\tilde{\mathbf{A}}_2)$. Of course, let these notations also apply to the Euclidean representation.

After some symbolic computations, it can be stated that the degenerate circles satisfy, either $\Sigma(\lambda_+) = 2$ *and* $\Sigma(\lambda_-) = \Sigma(\lambda_3) = 1$ for concentric generators, or $\Sigma(\lambda_+) = \Sigma(\lambda_-) = 2$ *and* $\Sigma(\lambda_3) = 0$, otherwise. Thanks to invariance of the absolute signature, this eventually entails that:

$$
\Sigma(\tilde{\mathbf{A}}_1 - \tilde{\lambda}_\pm \tilde{\mathbf{A}}_2) \geq 1 \geq \Sigma(\tilde{\mathbf{A}}_1 - \tilde{\lambda}_3 \tilde{\mathbf{A}}_2).
$$
(8)

The pair (d, r) ***as a double invariant of two circles.*** Assume that the $\tilde{\lambda}$'s in $\tilde{\boldsymbol{\lambda}}$ are sorted by decreasing order of absolute signatures such that (8) holds. As a result, d and r, given as functions (7) of the $\tilde{\lambda}$'s, are *projectively invariant*.

Therefore, given $(\tilde{\mathbf{A}}_1, \tilde{\mathbf{A}}_2)$, we can deduce the relative position of $\mathcal{A}_1$ and $\mathcal{A}_2$, by determining which constraint on d and r holds.

4.3 Recovering the line at infinity

After analysing their decompositions into lines according to (2), the set of three degenerate circles of the pencil are made up of:

- the rank-1 line-circle $\mathtt{L}_\infty^2$ twice and the point-circle $\mathtt{O^I O^J}$ (concentric case),
- a rank-2 line-circle $\Delta\mathtt{L}_\infty$ and the point-circle $\mathtt{Z^I Z^J}$ twice (tangent case),
- a rank-2 line-circle $\Delta\mathtt{L}_\infty$ and two distinct point-circles $\mathtt{Z_c^I Z_c^J}$ (disjoint case),

where $\mathtt{O}$ is the origin. Points $\mathtt{Z}$ as well as line Δ will be specified in §4.3.

The issue is now to recover the line at infinity $\mathtt{L}_\infty$. The only relative positions that require investigations are cases of two non-concentric circles i.e., iff $d > 0$.

What the generalized eigenvectors of $(\tilde{\mathbf{A}}_1, \tilde{\mathbf{A}}_2)$ ***tell us.*** Assume $d > 0$. MAPLE computes the matrix of generalized eigenvectors associated with $\tilde{\boldsymbol{\lambda}}$ as:

$$
\tilde{\mathbf{Z}} = \mathbf{HZ} \begin{pmatrix} \xi_1 & & \\ & \xi_2 & \\ & & \xi_3 \end{pmatrix}, \quad \mathbf{Z} = \begin{bmatrix} \frac{1+d^2-r^2+\sqrt{\beta}}{2d} & \frac{1+d^2-r^2-\sqrt{\beta}}{2d} & 0 \\ 0 & 0 & 1 \\ 1 & 1 & 0 \end{bmatrix},
$$
(9)

where ξ_1, ξ_2, ξ_3 are some non-zero scale factors.

The third column $\mathbf{z}_3$ of $\mathbf{Z}$ is the Euclidean vector of the centre of a line-circle ΔL_∞, with Euclidean matrix $\mathbf{A}(\lambda_3)$. Using (2), given that $\mathbf{l}_\infty \sim (0,0,1)^\top$, we have $\mathbf{A}(\lambda_3) \sim \mathbf{A}_1 - 1\mathbf{A}_2 \sim \mathbf{l}_\infty \boldsymbol{\delta}^\top + \boldsymbol{\delta}\mathbf{l}_\infty^\top$, where:

$$\boldsymbol{\delta} = (-2d, 0, 1 + d^2 - r^2)^\top. \tag{10}$$

$\boldsymbol{\delta}$ is the Euclidean vector of the **radical axis** Δ of $\{\mathcal{A}_1, \mathcal{A}_2\}$, which is the locus of points having equal powers w.r.t. both circles [5, pp. 95-96]. Note that when $d = 0$, we have $\boldsymbol{\delta} \sim \mathbf{l}_\infty$ so $\Delta L_\infty = L_\infty^2$ consists of the repeated line at infinity.

Vectors $\mathbf{z}_c$ ($c = 1, 2$) are the Euclidean vectors of the centres Z_c of point-circles $Z_c^\text{I} Z_c^\text{J}$, whose Euclidean matrices are $\mathbf{A}(\lambda_c)$. A point-circle $Z_c^\text{I} Z_c^\text{J}$ may be looked upon a "limiting circle" of the pencil with radius zero. For this reason, Z_c is called a **limiting point** of the pencil $\{\mathcal{A}_1, \mathcal{A}_2\}$ [5, p.97] (see Fig. 2). If $\mathcal{A}_1$, $\mathcal{A}_2$ are separate, then it is defined as the point included in every circle of $\{\mathcal{A}_1, \mathcal{A}_2\}$ located in each half-plane bounded by Δ. If $\mathcal{A}_1$, $\mathcal{A}_2$ are tangent, both limiting points coincide with the contact point Z. In any case, they are located on the line of the centres of the generators.

An important fact is that vectors $\mathbf{z}_1$, $\mathbf{z}_2$ satisfy $(\boldsymbol{\delta}^\top \mathbf{z}_1)(\boldsymbol{\delta}^\top \mathbf{z}_2) \leq 0$ i.e., that Z_1 and Z_2 either *lie on the radical axis Δ or are on opposite sides of* Δ. Since $(\mathbf{l}_\infty^\top \mathbf{z}_1)(\mathbf{l}_\infty^\top \mathbf{z}_2) > 0$, they also lie *on the same half-plane bounded by* L_∞.

5 Outline of the proposed algorithm

We will now make again the distinction between the entities of π and their projections onto the image plane $\tilde{\pi}$, by adding ˜ to the calligraphic letters denoting these latter. Thus, let us denote by $\tilde{\mathbf{A}}_j$, $j = 1..N$, the image matrices of the projections $\tilde{\mathcal{A}}_j$ of N circles $\mathcal{A}_j$ of π, onto the image plane $\tilde{\pi}$.

The proposed algorithm consists in "fitting" the projection $\widetilde{\text{IJ}}$ of the circular-point envelope IJ, using constraints (3a-3c), from the degenerate projected circles of the pencils $\{\tilde{\mathcal{A}}_1^q, \tilde{\mathcal{A}}_2^q\}$ spanned by Q selected pairs, $1 \leq q \leq Q \leq \frac{1}{2}N(N-1)$. To estimate the matrix $\tilde{\mathbf{C}}_\infty^*$ of $\widetilde{\text{IJ}}$ with a linear method, we substitute some regular symmetric matrix $\mathbf{X}$ for $\tilde{\mathbf{C}}_\infty^*$ in Eqs. (3a-3c). Hence, there are six unknowns, defined up to a scalar. The algorithm works as follows. We solve the equation system built by calling the procedure **AddLinearConstraint**(), as described in Procedure 1, for each of the Q matrix-pairs $(\tilde{\mathbf{A}}_1^q, \tilde{\mathbf{A}}_2^q)$. Basically, this procedure identifies the relative position of the corresponding circles in π and classifies the degenerate members of $\{\tilde{\mathcal{A}}_1^q, \tilde{\mathcal{A}}_2^q\}$, so as to yield equations (3a) and/or (3b).

Note that our solution generalizes that of Liebowitz [10, p.56][14, p.60], by the ability of also treating simultaneously pairs of projected orthogonal lines i.e., enabling us to add constraints (3c).

N=2 projected circles (exact solution). Given one pair $(\tilde{\mathbf{A}}_1^q, \tilde{\mathbf{A}}_2^q)$ we can obtain zero or one constraint (3a) and two constraints (3b). For problem P_2 to be well-posed so to get an exact solution, we need at least one constraint (3a), ensuring that the property $\text{rank}(\mathbf{X}) = 2$ holds, plus at least one constraint (3b). We have to discuss in which cases this can be achieved. Remind that the

projected line-circle $\widetilde{\mathsf{L}_\infty \Delta^q}$ can always be identified among the three degenerate circles of the pencil $\{\tilde{\mathcal{A}}_1^q, \tilde{\mathcal{A}}_2^q\}$ *but* there is an ambiguity in saying which line is $\tilde{\mathsf{L}}_\infty$ (or, equivalently, the projected radical axis $\tilde{\Delta}^q$). Since, in the world plane, the limiting points Z_1^q, Z_2^q of a pencil $\{\mathcal{A}_1^q, \mathcal{A}_2^q\}$ either lie on, or are on both sides of, the radical axis Δ^q (cf. §4.3), we claim that (superscript q is omitted):

Proposition 1. *A necessary and sufficient condition for the projected limiting points $\tilde{\mathsf{Z}}_1$, $\tilde{\mathsf{Z}}_2$ to lie, in the image plane, on opposite sides of the projected radical axis $\tilde{\Delta}$ is that Z_1, Z_2 lie, in the world plane π, on the same half-plane bounded by the line $(\pi \cap \tilde{\pi}_F)$, which is the intersection of the principal plane[6] $\tilde{\pi}_F$ and π.*

Proof is omitted due to lack of space. Note that this proposition (see Fig. 2) could have been equivalently stated by using a condition for $\tilde{\mathsf{Z}}_1$ and $\tilde{\mathsf{Z}}_2$ to lie, in the image plane, on the same half-plane bounded by $\tilde{\mathsf{L}}_\infty$.

In other words, we know exactly when P_2 is well-posed: the Euclidean structure can be recovered from two projected circles, providing the limiting points lie in front of the camera. This holds for all relative positions of two circles except for some, *not all*, cases of enclosing, non-concentric, circle-pairs. Clearly, there exist such pairs (see Fig. 2) from which $(\tilde{\mathsf{I}}, \tilde{\mathsf{J}})$ is recoverable, contrary to what was claimed in some previous works [11][23].
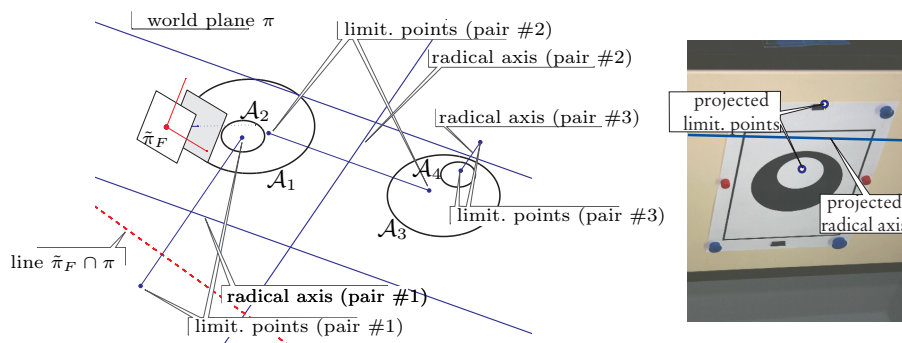
Fig. 2. Prop. 1 says that problem P_2 is ill-posed for enclosing pair #1 $(\mathcal{A}_1, \mathcal{A}_2)$ but well-posed for separate pair #2 $(\mathcal{A}_1, \mathcal{A}_3)$ and enclosing pair #3 $(\mathcal{A}_3, \mathcal{A}_4)$. Right-hand, a real image of some enclosing pair, from which the projected circular points are recovered.

*$N{\geq}2$ **projected circles (Least-Squares solutions).*** If $N \geq 2$, strictly speaking, this is an overdetermined problem of estimating parameters subject to an ancillary constraint, in our case $\det(\mathbf{X}) = 0$. Efficient and well-founded methods exist, e.g. [4]. However, we use a straightforward solution that consists in seeking a least-squares solution $\hat{\mathbf{X}}$, then imposing the ancillary constraint via a rank-2 approximation of $\hat{\mathbf{X}}$ by cancelling its smallest singular value.

---

[6] Containing the camera centre and parallel to the image plane.

It is worth noting that, once the circular point-envelope is recovered, a rectifying homography matrix $\mathbf{M}^{-1}$ can be computed [10, pp.55-56] from the SVD-like decomposition $\tilde{\mathbf{C}}^*_\infty = \mathbf{M}\,\mathrm{diag}(1,1,0)\mathbf{M}^\top$, where $\mathbf{M} \in \mathbb{R}^{3\times 3}$ satisfies $\mathbf{M} \sim \mathbf{HS}$ for some 2D similarity $\mathbf{S} \in \mathbb{R}^{3\times 3}$ of π. Since there are only 4 d.o.f. in $\tilde{\mathbf{C}}^*_\infty$, there are also only 4 d.o.f. in $\mathbf{M}$. Typically, by applying $\mathbf{M}^{-1}$ to the image, we get its metric rectification (e.g., as shown in Fig. 4).

5.1 Non-Linear Optimization.

We also implemented a bundle adjustment style optimization of both, the rectified circles, and the plane-to-image homography. In addition, for every image point we estimate an associated point that lies exactly on the associated rectified circle. The cost function for the optimization is then the sum of squared distances between image points and corresponding points on circles, re-projected to the image via the homography.

Since rectification is defined up to a similarity transformation in the scene plane, we may fix 4 degrees of freedom in our parameterization. We implemented two approaches to do so. The first one is to parameterize the homography using 4 parameters [10]. The second one is to use 8 parameters for the homography (we simply fix H_{33} to a non-zero value, which is appropriate in our scenario), but to fix the centres of two of the circles to their initial positions.

Each circle $\mathcal{A}_c$ is naturally parameterized by its radius r_c and centre (x_c, y_c), and each point Q_{cp} on a circle is parameterized by an angle Θ_{cp}, with vector $\mathbf{Q}_{cp} = (x_c + r_c \cos\Theta_{cp}, y_c + r_c \sin\Theta_{cp}, 1)^\top$. The optimization problem is then:

$$\min_{\mathbf{H}, x_c, y_c, r_c, \Theta_{cp}} \sum_{c=1}^{N} \sum_{p=1}^{P} dist^2(\mathbf{q}_{cp}, \mathbf{HQ}_{cp})$$

The initializations of the unknowns is rather trivial, given the results of a rectification with any of the method LINEAR. Note that with the above cost function is identical in spirit to the one used in [8] for estimating ellipses that minimize the sum of squared distances to data points.

We use Levenberg-Marquardt for the optimization, and take advantage of the sparse structure of the Jacobian. The most complex step in each iteration is the inversion of a symmetric matrix of order $(4 + N)$. Typically, for simulated experiments similar to those in §6, with up to $N = 10$ circles and 50 points per circle, the optimization took (much) less than a second (see results in Tab. 1)

Circles	2	3	4	5	6	7	8	9	10
RMS	0.49	0.52	0.54	0.55	0.56	0.57	0.57	0.57	0.58

Table 1. RMS residuals of non-linear optimization. Average over 500 runs of the square roots of the average cost function value.

Procedure 1   SYS = **AddLinearConstraint**(SYS, $\tilde{\mathbf{A}}_1$, $\tilde{\mathbf{A}}_2$)

```
[ λ̃,  Z̃ ] = GeneralizedEig(Ã₁, Ã₂)
if all λ̃'s are real /* non-interesecting circles only */  then
  sort λ̃ and Z̃ to ensure Σ(Ã(λ̃ₖ)) ≥ Σ(Ã(λ̃ₗ)) for k ≤ l
  compute d and r using (7)
  if d == 0 /* concentric circles */  then
    l̃∞ = Ã₁z̃₁
    add equation (3a) to system SYS /* affine constraint */
    [ x̃₁,  x̃₂ ] = LinesofRank2RealConic(Ã₁ − λ̃₁Ã₂) /* Σ == 2 */
    add equation (3b) to system SYS /* Euclidean constraint */
  else
    if d ≥ |r − 1| /* non-enclosing circles only */  then
      [ l₀,  l₁ ] = LinesofRank2RealConic(Ã₁ − λ̃₃Ã₂) /* Σ == 0 */
      l̃∞ = l₁₋c, where c ∈ {0,1} is such that (1/(Z̃₃₁Z̃₃₂))(lₒᵀz̃₁)(lₒᵀz̃₂) < 0
      add equation (3a) to system SYS /* affine constraint */
    end if
    for k ∈ {1..2} do
      [ x̃₁,  x̃₂ ] = LinesofRank2RealConic(Ãₖ − λ̃ₖÃ₂) /* Σ == 2 */
      add equation (3b) to system SYS /* Euclidean constraint */
    end for
  end if
end if
```

---

6   Experiments

Synthetic data. We are aiming here at assessing how accurately is fitted the Euclidean structure, given $N = 16$ unknown non-intersecting circles projected in one view. We investigate the link between the number $Q \in \{1, .., 25\}$ of randomly selected circle-pairs (among the 120 possible pairs) and several fitting errors. Fig. 3 shows the average values of these errors.

The synthetic scene, located on some world-plane π, consists of a 1500×1500 square area over which are spatially distributed the N circles, whose radii vary within $[25; 75]$. The camera is at a distance of about 2500, with randomly generated camera orientations, in terms of azimuth, elevation and swing angles varying within $[-60°; 60°]$. The simulated camera has a 512×512 pixel resolution and constant internal parameters. Note that the "true" world-to-image homography $\mathbf{H}$, induced by the chosen Euclidean representation of π, must obey to the decomposition [20][24] $\mathbf{H} = \mathbf{K}\mathbf{R}\,[\,\mathbf{e}_1 \mid \mathbf{e}_2 \mid \mathbf{t}\,]$, where $\mathbf{K} \in \mathbb{R}^{3\times 3}$ is the calibration matrix, $\mathbf{R} \in \mathbb{R}^{3\times 3}$ is the rotation describing the orientation of π w.r.t. the camera frame, with $\mathbf{r}_3$ as normal to π; $\mathbf{t} \in \mathbb{R}^3$. Hence, the "true" projected circular-point envelope $\tilde{\mathbf{C}}^*_\infty$ satisfies $\mathbf{K}^{-1}\tilde{\mathbf{C}}^*_\infty\mathbf{K}^{-\top} \sim \mathbf{R}\,\mathrm{diag}(1,1,0)\mathbf{R}^\top$ i.e., its two nonzero singular values are equal.

Each circle projects to an ellipse, sampled by S equally spaced pixels, where S roughly equals the ellipse perimeter. Gaussian noise of zero mean and standard deviation $\sigma = 1$ is added to the pixel (integer) coordinates. Series of 500 tests are conducted for each of the following error criteria.

Let $\hat{\mathbf{C}}_\infty^*$ denote the estimation of $\tilde{\mathbf{C}}_\infty^*$, using our algorithm described in §5, both matrices normalized to have unitary Frobenius norm. Referring to Fig. 3(a), two error criteria on $\hat{\mathbf{C}}_\infty^*$ are derived. We quantify, in a way, how $\hat{\mathbf{C}}_\infty^*$ is closed to the "true" $\tilde{\mathbf{C}}_\infty^*$: first, by computing the relative error $(\hat{s}_1 - \hat{s}_2)/\hat{s}_1$, where $\hat{s}_1 \geq \hat{s}_2 > \hat{s}_3 = 0$ are the singular values of $\mathbf{K}^{-1}\hat{\mathbf{C}}_\infty^*\mathbf{K}^{-\top}$, involving the "true" $\mathbf{K}$ ("*singular value constraint*"); second, by computing the error $||\hat{\mathbf{C}}_\infty^* - \tilde{\mathbf{C}}_\infty^*||_F$ ("*Frobenius norm*"). In Fig. 3(b), we quantify the error on the pose of π, by computing the *angular error on the plane's normal*, that is $\arccos(\mathbf{r}_3^\top \hat{\mathbf{u}}_3)$, involving the "true" $\mathbf{r}_3$, where $\hat{\mathbf{u}}_3$ is the singular vector associated with $\hat{s}_3 = 0$.

Let $\hat{\mathbf{M}}^{-1}$ be the estimated rectifying homography, obtained from $\hat{\mathbf{C}}_\infty^*$ (cf. end of §5). In Fig. 3(c-d), we assess the accuracy of the 2D reconstruction by computing errors on the alignment between reconstructed of image points, via $\hat{\mathbf{M}}^{-1}$, and true world points. The alignment error is the sum of the squared residuals for all points, from the best Euclidean 2D mapping between reconstructed points and true points. Alignment errors have been computed for the circle points and circle centres as well as for a set of control points. Lastly, in Fig. 3(d), we compute the relative error on "normalized" radii and distances between centres, as defined by r and d in §4.2, of the (approximated) reconstructed circles.

These series of tests show the excellent performance of the proposed algorithm. The obtained solutions are unquestionably more stable when using multiple circles, much like using more than multiple points to fit a conic.

Real data. We illustrate the performance of the proposed algorithm by carrying out a metric rectification [10, §1.7.5] of 3D planes i.e., by warping the image to remove the perpespective distortion. The images in Fig.4 was captured using a CANON EOS 300D camera, with 1536×1024 image resolution.

7   Conclusion

We described a method for recovering the Euclidean structure of some observed world plane π, from $N \geq 2$ projected parallel circles. We suggested to state the problem as that of "fitting" the projected degenerate absolute conic of π, namely the projected circular-point envelope $\widetilde{\mathtt{IJ}}$, to line-pairs, so-called projected line- and point-circles. These are the degenerate members of the conic pencil, spanned by all (or some) combinations of pairs of the whole set of projected circles. We showed that the degenerate members of the pencil can yield either affine or Euclidean linear constraints on the parameters of $\widetilde{\mathtt{IJ}}$. Depending on the relative position of the corresponding circle-pair in π, we show exactly what these line-pairs are and which kind of constraints they will set on $\widetilde{\mathtt{IJ}}$. Consequently, the problem is stated as that of solving a (possibly) overdetermined system of linear equations, so taking into account more than two projected circles.

We are convinced that the usefulness of the proposed formalism, through the interpretation of the geometrical nature of the degenerate members of conic pencils or quadric pencils, as reported in [17], might go beyond the scope of this work e.g., regarding calibration of catadioptric cameras [2], or even the problem of calibration from spheres [1].
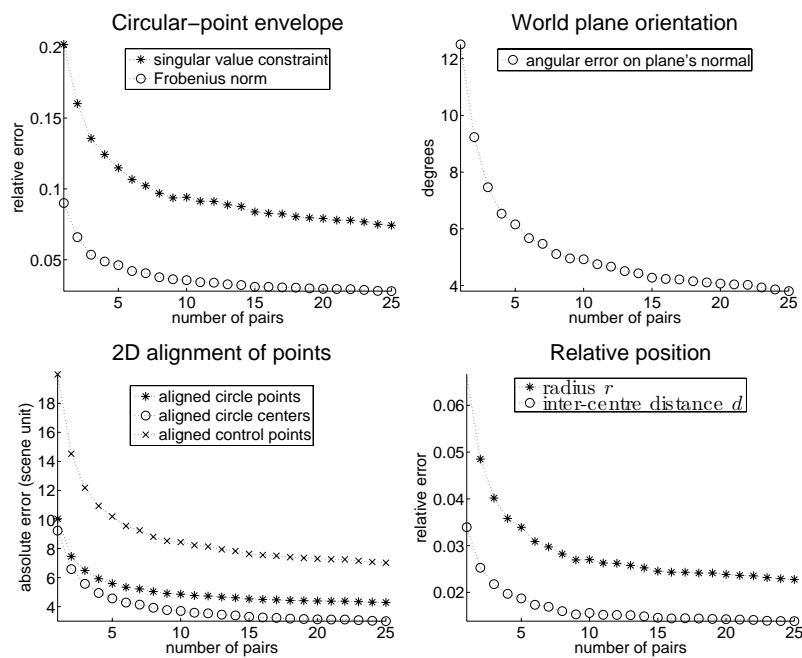
Fig. 3. Assessing the performance of the proposed method.
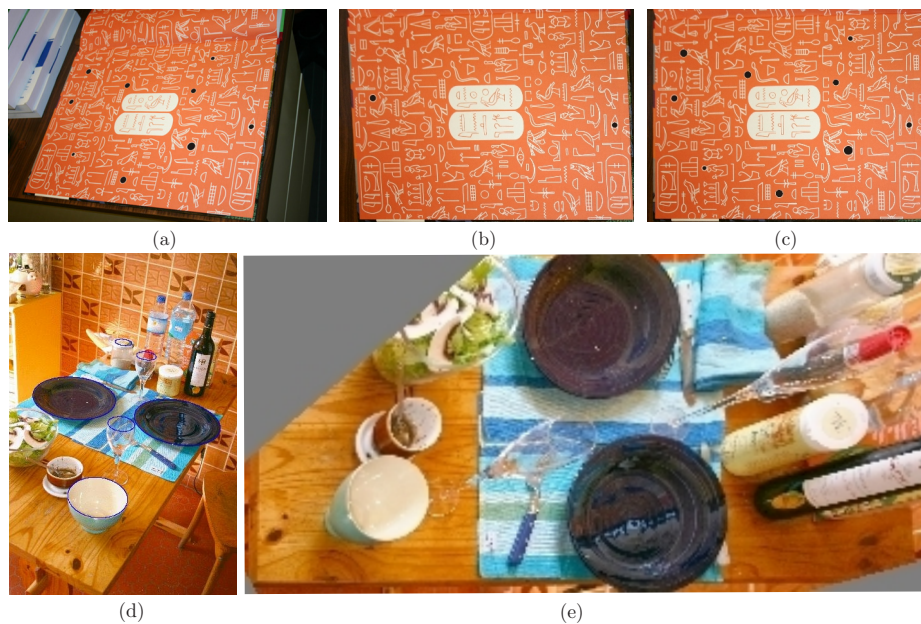
Fig. 4. *Top: (a) 1536×1024 photograph of the endpaper of some comic book, with drawn hieroglyphs. (b) Image rectification from $N = 2$ (black-filled) circles ; (c) from $N = 9$ circles. Bottom: (d) 1536×1024 photograph of a table in a kitchen, (e) Image rectification (cropped) using $N = 6$ (blue) circles.*

14

References

1. M. Agrawal and L.S. Davis, "Camera calibration using spheres: A semi-definite programming approach," *ICCV,* vol. 2, pp. 782-791, 2003.
2. J. Barreto, General Central Projection Systems: Modeling, Calibration and Visual Servoing. Ph.D. Thesis. University of Coimbra. 2003.
3. Q. Chen, H. Wu and T. Wada, "Camera Calibration with Two Arbitrary Coplanar Circles," *ECCV,* vol. 3, pp. 521-532, 2004.
4. W. Chojnacki, M.J. Brooks, A. van den Hengel and D. Gawley, "A New Constrained Parameter Estimator for Computer Vision Applications," *IVC,* vol. 22(2), pp. 85-91, 2004.
5. J.-L. Collidge, *A Treatise on the Circle and the Sphere.* Oxford: Clarendon Press, 1916.
6. C. Columbo, A. Del Bimbo and F. Pernici, "Metric 3D Reconstruction and Texture Acquisition of Surfaces of Revolution from a Single Uncalibrated View," *PAMI,* vol. 27, no. 1, pp. 99-114, Jan. 2005.
7. A.W. Fitzgibbon, M. Pilu, and R.B. Fisher, "Direct Least Square Fitting of Ellipses," *PAMI,* vol. 21, no. 5, pp. 476-480, May 1999.
8. W. Gander, G.H. Golub and R. Strebel, "Fitting of Circles and Ellipsess," *BIT*, 34, pp.558-578, 1994.
9. G. Golub and C. Van Loan, *Matrix Computations.* Johns Hopkins University Press, 3rd edition, 1996.
10. R. Hartley and A. Zisserman, *Multiple View Geometry in Computer Vision.* Cambridge Univ. Press, 2nd edition, 2003.
11. G. Jiang, H.-T. Tsui, L. Quan, and A. Zisserman, "Single Axis Geometry by Fitting Conics," *ECCV,* vol. 1, pp. 537-550, May 2002.
12. K. Kanatani and W. Liu, "3D Interpretation of Conics and Orthogonality," *CVIU,* vol. 58, no. 3, pp. 286-301, Nov. 1993.
13. J.-S. Kim, P. Gurdjos and I.-S. Kweon, "Geometric and Algebraic Constraints of Projected Concentric Circles and Their Applications to Camera Calibration," *PAMI,* vol. 27, no. 4, pp. 637 - 642, April 2005.
14. D. Liebowitz, Camera Calibration and Reconstruction of Geometry from Images. Ph.D. Thesis University of Oxford. Trinity Term 2001.
15. S.D. Ma, "Conics-based Stereo, Motion estimation, and Pose Determination," *IJCV,* vol. 10, no. 1, pp. 7-25, Feb. 1993.
16. J.L. Mundy and A. Zisserman Eds., *Geometric Invariance in Computer Vision* MIT Press, 1992.
17. L. Quan, "Conic Reconstruction and Correspondence from Two Views," *PAMI,* vol. 18, no. 2, pp. 151-160, Feb. 1996.
18. J. Semple and G. Kneebone, *Algebraic Projective Geometry.* Oxford Classic Series, 1952, reprinted, 1998.
19. P. Sturm and L. Quan, "Affine Stereo Calibration," Technical Report LIFIA-29, LIFIA-IMAG, June 1995.
20. P. Sturm and S. Maybank, "On Plane-Based Camera Calibration: a General Algorithm, Singularities, Applications," *CVPR,* vol. 1, pp. 1432-1437, 1999.
21. B. Triggs, "Autocalibration and the Absolute Quadric," *CVPR,* pp. 609-614, 1997.
22. B. Triggs, "Autocalibration from Planar Scenes," *ECCV,* vol. 1, pp. 89-105, 1998.
23. Y. Wu, X. Li, F. Wu and Z. Wu, "Coplanar circles, Quasi-Affine Invariance and Calibration," *Image and Vision Computing.* To appear, 2004.
24. Z. Zhang, "A Flexible New Technique for Camera Calibration," *PAMI,* vol. 22, no. 11, pp. 1330-1344, Nov. 2000.